Regio- and Enantioselective Macrocyclization from Dynamic Imine Formation: Chemo- and Enantioselective Fluorescent Recognition of Lysine

Yifan Mao, Stephanie Davis, and Lin Pu*

Department of Chemistry, University of Virginia, Charlottesville, Virginia 22904, USA. E-mail: lp6n@virginia.edu

Received Date (will be automatically inserted after manuscript is accepted)

The dynamic covalent chemistry of imines is utilized to conduct a regioselective as well as enantioselective synthesis of an unsymmetric (C_1) chiral macrocycle from the reaction of an unsymmetric (C_1) chiral dialdehyde (*S*)-**4** that contains a salicylaldehyde unit and a benzaldehyde unit, with lysine, an unsymmetric (C_1) chiral diamine. The enantioselectivity is further enhanced in the presence of Zn^{2+}. Compound (*S*)-**4** in combination with Zn^{2+} is found to be a highly chemoselective as well as enantioselective fluorescent probe for lysine. It can be used to detect the specific enantiomers of this amino acid.

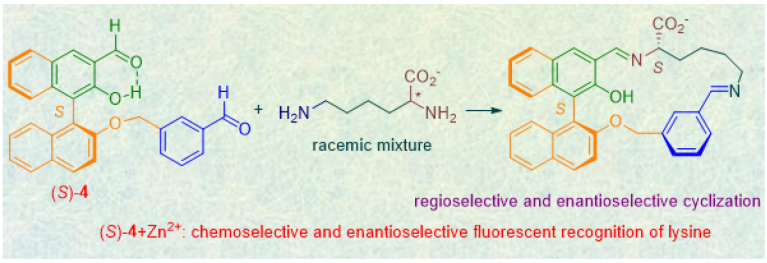

The dynamic covalent chemistry of imines has been actively utilized in the construction of materials of diverse structures such as macrocycles, cages, polymers, and covalent organic networks.[1-5] The reversible formation of imines from aldehydes and amines and the subsequent transiminations have allowed the development of many highly selective reaction processes for materials synthesis. C_2 and C_3 symmetric chiral diamines and triamines have been used to react with symmetric and achiral di- or polyaldehydes to make chiral macrocycles and cages.[6-8] Symmetric chiral dialdehydes have also been reacted with symmetric chiral diamines to make chiral macrocycles.[9-11] For example, a racemic C_2 symmetric chiral dialdehyde **1** was found to react with one enantiomer of the C_2 symmetric chiral diamine **2** to generate a D_2 symmetric chiral macrocycle **3** for the chirality-matched partners and a polymer for the mismatched ones (Scheme 1).[9] That is, an enantioselective condensation took place to give the chiral macrocyclic product. In all of the previous studies on chiral macrocycles and cages formed from the dynamic covalent chemistry of imines, the symmetries of both aldehydes and amines are important in order to avoid the formation of a mixture of unsymmetric regioisomers. No reaction was reported with both regio- and enantiocontrol to produce unsymmetric (C_1) chiral macrocycles or cages from the condensation of unsymmetric (C_1) chiral polyamines with unsymmetric (C_1) chiral polyaldehydes.

Scheme 1. An enantioselective reaction of a C_2 symmetric chiral dialdehyde with a C_2 symmetric chiral diamine.

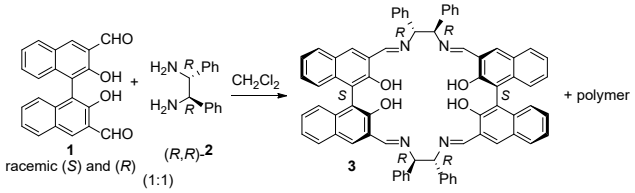

In order to diversify the structures of the materials that can be generated from the dynamic imine chemistry, we have proposed to develop regioselective as well as enantioselective processes to form unsymmetric chiral macrocycles from unsymmetric chiral aldehydes and amines. An unsymmetric chiral dialdehyde (*S*)-**4** is thus designed which contains two different types of aldehyde units, one structurally similar to salicylaldehyde and another similar to benzaldehyde (Figure 1). It is known that the reaction of salicylaldehyde with amines proceeds much faster with greater conversion than that of benzaldehyde because of its intramolecular hydrogen bond.[12] The resulting imines from salicylaldehyde are also more stable than those from benzaldehyde due to a strong intramolecular hydrogen bond between the imine nitrogen and the adjacent hydroxyl proton. We have investigated the reaction of this unsymmetric chiral dialdehyde with lysine (Lys), an unsymmetric chiral diamine. Because of both steric and electronic factors, the ε-amine group of Lys should be more reactive with aldehydes than the α-amine group under basic conditions. The distinctively different reactivity of the two aldehyde groups of (*S*)-**4**, that of the two amine groups of Lys, and the different stability of the resulting imines might provide biased reaction pathways to direct a selective product formation. We have discovered a highly regioselective as well as enantioselective process from the reaction of (*S*)-**4** with L- and D-Lys. We have further found that the enantioselectivity for the reaction of (*S*)-**4** with racemic Lys can be enhanced in the presence of Zn^{2+}. In addition, (*S*)- or (*R*)-**4** in combination with Zn^{2+} has exhibited chemoselective as well as enantioselective fluorescent recognition of Lys among common amino acids. It can be used to detect the specific enantiomer of this amino acid. Herein, these results are reported.

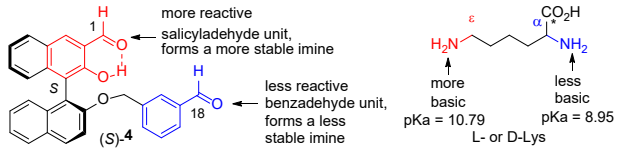

Figure 1. Design of an unsymmetric chiral dialdehyde (*S*)-**4** and features of Lys.

Compound (*S*)-**4** is readily synthesized according to Scheme S1.[13] The ^{1}H NMR spectrum of (*S*)-**4** in DMSO-d_6 shows its two

aldehyde signals at δ 10.34 (proton 1) and 9.76 (proton 18). The intramolecular hydrogen bonding with the ortho hydroxyl group has shifted the proton 1 signal of the salicylaldehyde unit of (*S*)-**4** more down-field than that of the benzaldehyde unit. This hydrogen bonding also leads to a highly down-field shifted hydroxyl signal at δ 10.23 (See Figure S1-S8 in SI for the NMR spectra).

We first studied the reaction of (*S*)-**4** with the sodium salt of L-Lys, L-Lys$^-$, prepared from the reaction of L-Lys with NaOH (1.0 equiv) in methanol followed by evaporation. Figure 2 gives the ^{1}H NMR spectra of (*S*)-**4** with 0 – 2 equiv L-Lys$^-$ in DMSO-d_6 at room temperature for 6 h (for the reactions with 0 – 8.0 equiv L-Lys$^-$, see Figure S9 in SI). It shows that at 2.0 equiv L-Lys$^-$, the reaction has generated almost a single product. On the basis of a series of 1D and 2D NMR spectra including ^{1}H, ^{13}C, HSQC, COSY, TOCSY and NOESY (See Figure S10 – S19 for detailed signal assignment), a macrocyclic structure **6** is established for this product. The two imine proton signals of **6** are observed at δ 8.62 (proton 1) and 8.13 (proton 18). An NOE effect is observed between the imine proton 1 and the α-proton 23 (δ 3.63) and between the imine proton 18 and the ε-protons 19 (δ 3.53) (Figure S14 in SI). The TOCSY spectrum (Figure S13 in SI) shows a correlation between the α-proton 23 and the ε-protons 19 which confirms the macrocyclic structure. In the TOF mass spectrum (ES+), a peak at m/z = 543.2277 is observed for **6** (calcd for **6**+2H: 543.2278) (Figure S20 in SI).

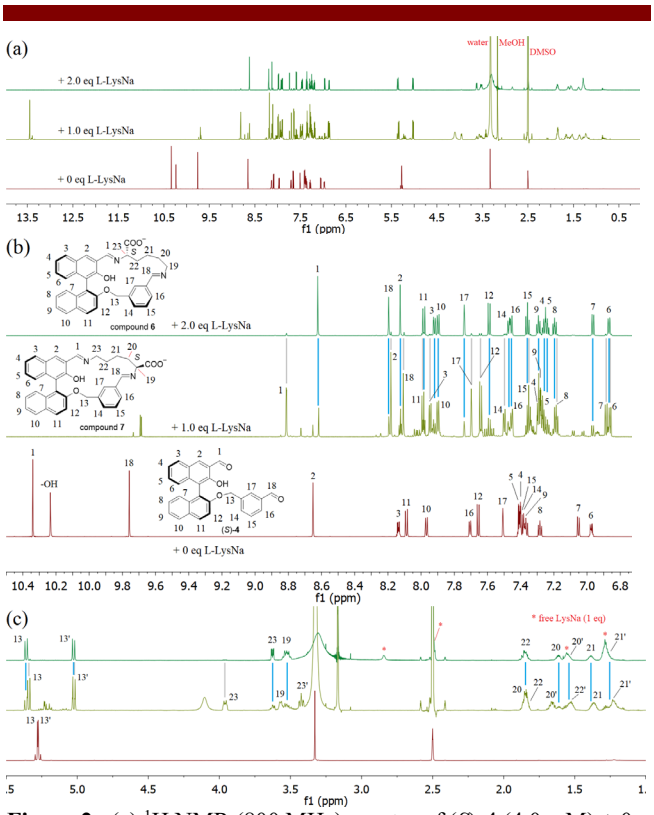

Figure 2. (a) ^{1}H NMR (800 MHz) spectra of (*S*)-**4** (4.0 mM) + 0 - 2.0 equiv L-Lys$^-$ in DMSO-d_6. (Reaction time: rt for 6 h). (b) and (c) zoomed regions with signal assignments.

In the ^{1}H NMR spectrum of the reaction of (*S*)-**4** with 1.0 equiv L-Lys$^-$ shown in Figure 2, the major product is assigned to another macrocycle **7** and the minor product to **6** on the basis of the 2D NMR spectra HSQC, COSY, TOCSY and NOESY (see Figure S21-S28 in SI for detailed signal assignment). Compounds **6** and **7** are regioisomers. The two imine protons of **7** are observed at δ 8.81 (proton 1) and 8.10 (proton 18). The macrocyclic structure is established by the correlation of these two imine protons with the protons 23 and 19 by NOESY and TOCSY spectra. The peak at δ 13.45 can be assigned to the hydroxyl protons of both **7** and **6**. This hydroxyl signal is much more down-field than that of (*S*)-**4**, indicating significantly stronger intramolecular hydrogen bonds in the imine products than that in the aldehyde. In the presence of an excess amount of L-Lys$^-$ (2.0 equiv), **7** is almost completely converted to **6**. The excess L-Lys$^-$ should also catalyze the rapid exchange of the hydroxyl proton, leading to the disappearance of the hydroxyl signal at δ 13.45.

In the TOF mass spectrum (ES+) of the reaction mixture of (*S*)-**4** with 1.0 equiv L-Lys$^-$, a peak at m/z = 543.2286 is observed for both **7** and **6** (calcd for **7** or **6**+2H: 543.2278) (Figure S29 in SI). Two peaks at m/z = 561.2390 and 531.2285 are observed for the monoaldehyde intermediate **8**+2H (calcd: 561.2389) and **8**+2H-HCO (calcd: 531.2284) respectively. Formation of the monoaldehyde intermediate **8** is also supported by the ^{1}H NMR spectrum of (*S*)-**4** +1.0 equiv L-Lys$^-$ in Figure 2 which shows the disappearance of the salicylaldehyde signal of (*S*)-**4** at δ 10.34 with a small benzaldehyde signal remaining at δ 9.73.

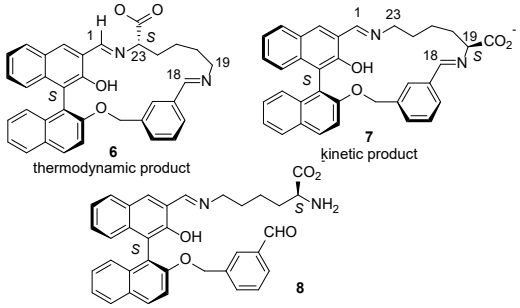

We monitored the reaction of (*S*)-**4** with 2.0 equiv L-Lys$^-$ from 10 min to 6 h by ^{1}H NMR spectroscopy (Figure S30 and S31 in SI). It was found that in 10 min, (*S*)-**4** was completely converted to **7** (major) and **6** (minor). The reaction reached equilibrium in 6 h with the formation of **6** (93.5%) and **7** (6.5%). This demonstrates that compound **7** is the kinetic product that forms faster and then converts to **6**. That is, the reaction of (*S*)-**4** with L-Lys$^-$ forms the thermodynamic product **6** with high regioselectivity.

The molecular modeling structures of **6** and **7** are obtained by conducting DFT calculation using Gaussian 16 program [B3LYP/6-31G+(d)(p)] (Figure S96). The calculation shows that **6** is more stable than **7** by 4 kcal/mol. The higher stability of **6** could be attributed to a possible intramolecular hydrogen bonding interaction between the carboxyl anion and the more acidic imine proton 1. Because of the intramolecular hydrogen bonding of the nitrogen atom of the imine 1 with the ortho-hydroxyl proton in **6**, the imine proton 1 should be more acidic than the imine proton 18. Thus, in the regioisomer **7**, the hydrogen bonding between the carboxylate group and the imine proton 18 should be much weaker.

On the basis of the above study, a mechanism for the reaction of (*S*)-**4** with L-Lys$^-$ is proposed in Scheme 2. When (*S*)-**4** is treated with L-Lys$^-$, the reaction of the more reactive salicylaldehyde unit of (*S*)-**4** with the more nucleophilic ε-NH$_2$ of L-Lys$^-$ to form **8** is expected to be the fastest step among the four competing amine-aldehyde condensations. The facile intramolecular condensation of **8** will generate the kinetic product **7**. The thermodynamic product **6** is generated from the intramolecular condensation of **9** formed from the condensation of the more reactive salicylaldehyde unit of (*S*)-**4** with the less reactive α-NH$_2$ of L-Lys$^-$ which forms a more stable imine unit due to its two possible intramolecular hydrogen bonding interactions. In both intermediates **8** and **9**, the less reactive benzaldehyde unit prefers to undergo the more favorable intramolecular reaction to form the macrocycles over the less favorable intermolecular reaction to form higher oligomers and polymers. Therefore, the different reactivity of the two aldehyde units of (*S*)-**4** and that of the two amine groups of L-Lys$^-$ together

with the stability difference of the products have led to the highly regioselective macrocyclization.

Scheme 2. Proposed Reaction Mechanism for (*S*)-**4** with L-Lys$^-$.

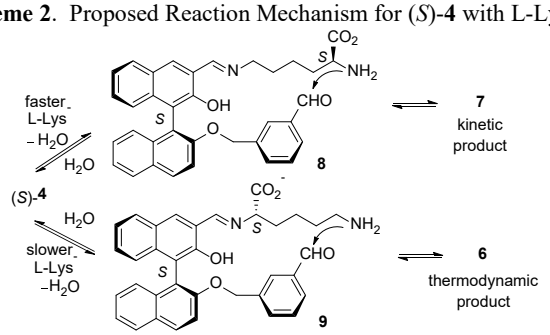

We also studied the reaction of (*S*)-**4** with D-Lys$^-$ (0 – 8 equiv) in DMSO-d_6 and the NMR spectra are shown in Figure S32-S36 in SI. When (*S*)-**4** is treated with 1.0 equiv D-Lys$^-$ at room temperature for 6 h, it forms a major product **10** whose structure is established on the basis of a series of 1D and 2D NMR studies (see Figure S37 - S44 in SI for detailed NMR signal assignment and HRMS spectrum). In the presence of 2.0 equiv D-Lys$^-$, (*S*)-**4** is completely converted to a mixture of **10** and **11** (see Figure S45 - S52 in SI for detailed 1D and 2D NMR signal assignment and HRMS spectrum). We monitored the reaction of (*S*)-**4** with 2.0 equiv D-Lys$^-$ from 10 min to 6 h by ^{1}H NMR spectroscopy (Figure S53 and S54 in SI). It was found that in 10 min, (*S*)-**4** was completely converted to **10** (major) and **11** (minor). The reaction reached equilibrium in 6 h with the formation of **10** (43.1%) and **11** (56.9%). Formation of the kinetic product **10** should be the result of the reaction of the more reactive salicylaldehyde unit with the more reactive ε-NH_2 group of D-Lys$^-$ which generates an intermediate like **8** as shown in Scheme 2 followed by its intramolecular condensation. Compound **11** is only slightly more stable than **10**, giving the observed final product mixture.

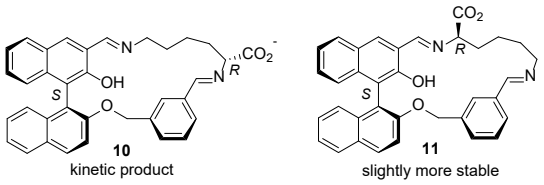

We have compared the reactivity of (*S*)-**4** with L-Lys$^-$ versus that with D-Lys$^-$ by monitoring the reaction of (*S*)-**4** with 2 equv racemic Lys$^-$. As shown in Figure S55 and S56, in 10 min, (*S*)-**4** is completely converted to a mixture of the 4 macrocyclic products **6**, **7**, **10** and **11**. The two kinetic products **7** and **10** were produced in about 1:1 ratio. The formation of the intermediate **8** from L-Lys$^-$ and that of its diastereomer from D-Lys$^-$ are expected to be of similar rates because the chiral center of the Lys unit is far away from the highly reactive salicylaldehyde unit. Then, the facile intramolecular condensations of **8** and its diastereomer to form the macrocycles lead to the observed non-enantioselective formation of the kinetic products. However, in the equilibrium mixture after 20 h, the enantioselective formation of the thermodynamic product from the reaction with L-Lys$^-$ is observed to give **6** as the major product in 67% yield.

The above results demonstrate that the reaction of (*S*)-**4** with Lys$^-$ is both regio- and enantioselective to form the unsymmetric chiral macrocycle **6**. This is the first example of such a process from the dynamic imine reaction.

The C_2 symmetric chiral dialdehyde (*S*)-**1** was found to undergo stereoselective reactions with amino acids in the presence of Zn^{2+}.[14] We have thus examined the effect of Zn^{2+} on the reaction of (*S*)-**4** with Lys. As shown in Figure S57, when the macrocycle **6**, generated from the reaction of (*S*)-**4** with L-Lys$^-$ (2.0 equiv) for 6 h, is treated with 1.0 equiv Zn^{2+}, the spectrum gives broad signals in which the two imine signals of **6** merges at δ 8.44. This indicates that the coordination of **6** with 1 equiv Zn^{2+} might generate interconverting structures (See Scheme S2 in SI for the proposed interconverting structures **12** and **13**). When more than 1.0 equiv Zn^{2+} is added, the merged imine signal at δ 8.44 is split into two signals which become stable at δ 8.61 and 8.18 in the presence of 4.0 equiv Zn^{2+} (Figure S57 and S58). The NMR spectra including NOESY and TOCSY spectra (Figure S59 – S66 in SI) have displayed correlations between the two imine proton signals through the adjacent protons 23 and 19. This demonstrates that the original macrocyclic structure of **6** is maintained in the Zn^{2+} complex. Excess Zn^{2+} should have saturated the coordination ability of the heteroatoms in the macrocycle to give the sharp signals for the final product with a tentatively proposed structure of **14**. In the mass spectrum (ES+) of the macrocycle **6** with excess Zn^{2+}, only the mono-Zn(II)-coordinated signal is observed at m/z = 623.1523 (calcd for **12**+H+H_2O: 623.1524) (Figure S67 and S68 in SI). No signal corresponding to the multi-Zn(II) coordination can be identified probably due to the instability of the coordination of the extra Zn^{2+} under the mass spectroscopic conditions. In spite of the efforts to grow single crystals for X-ray analysis, compound **14** was isolated only as powders with the incorporation of various solvent molecules (see Figure S94 and S95 in SI).

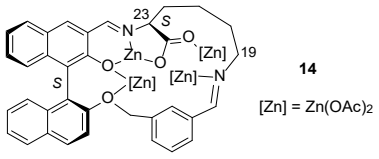

We also conducted ^{1}H NMR study on the reaction of (*S*)-**4** with D-Lys$^-$ in the presence of 0 – 4.0 equiv Zn^{2+}. As shown in Figure S69, when the 1:1.3 mixture of the macrocycles **10** and **11**, formed from the reaction of (*S*)-**4** with D-Lys$^-$ (2.0 equiv), is treated with 1.0 equiv Zn^{2+}, one major product is generated with two imine signals observed at δ 8.86 and 7.99 as confirmed by the HSQC spectrum (Figure S79 and S80 in SI). The NOESY and TOCSY spectra (Figure S76 – S78 in SI) show that the macrocyclic structures of **10** and **11** have opened to form a major product with a bis-D-Lys diimine structure represented by **15**. The two imine protons of **15** are not correlated in the 2D NMR spectra unlike those observed for the macrocycles discussed earlier. An NOE effect is observed between the imine proton 1 at δ 8.86 and the two diastereotopic protons 28 at δ 3.66 and 3.59; and between the imine proton 18 at δ 7.99 and the two diastereotopic protons 19 at δ 3.54 and 3.42 (See Figure S69 – S80 in SI for more detailed NMR assignments). When more than 1 equiv Zn^{2+} is added, all the signals become broad, indicating the formation of more complex structures such as oligomers and polymers. The TOF Mass (ES$^-$) spectrum of the reaction mixture of (*S*)-**4** + 2.0 equiv D-Lys$^-$ + 1.0 equiv Zn^{2+} in DMSO-d_6 shows the base peak at m/z = 659.147 for **15** (calcd for **15**-NH_2-H_2O-C_4H_8: 659.140) (Figure S81 in SI). Formation of compounds such as **15** shows that the macrocyclic structures generated from the reaction of (*S*)-**4** with D-Lys$^-$ are not stable in the presence of Zn^{2+}, and they open up to give the observed acyclic products.

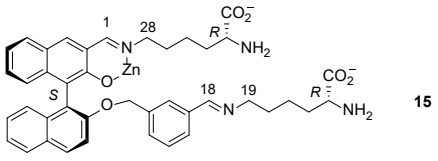

We further studied the reaction of (*S*)-**4** with racemic Lys$^-$ in the presence of Zn^{2+}. Figure S82 gives the ^{1}H NMR spectra for the addition of 0.25 – 4.0 equiv Zn^{2+} to the reaction mixture of (*S*)-**4** with racemic Lys$^-$ (2.0 equiv) that contains the macrocycle **6** as the major product from the regio- and enantioselective reaction of (*S*)-**4** with L-Lys$^-$. At 4.0 equiv Zn^{2+}, it shows the formation of the same final macrocyclic product as the reaction of (*S*)-**4** with L-Lys$^-$ and 4.0 equiv Zn^{2+}. No product from the reaction of (*S*)-**4** with D-Lys$^-$ and Zn^{2+} is observed.

The above experiment demonstrates that the enantioselectivity for the reaction of (*S*)-**4** with Lys$^-$ has been greatly enhanced with the addition of Zn^{2+}. That is, in the presence of Zn^{2+}, (*S*)-**4** only reacts with L-Lys$^-$ when treated with the 1:1 mixture of L- and D-Lys$^-$ to form a macrocyclic Zn^{2+} complex with high regio- and enantioselectivity.

Previously, we found that the C_2 symmetric dialdehyde (*S*)- or (*R*)-**1** shows enantioselective fluorescence enhancement with amino acids in the presence of Zn^{2+}.[15] Although the imines formed from the condensation of (*R*)-**1** with amino acids are not florescent, addition of Zn^{2+} turns on the enantioselective fluorescence.[15,16] Our discovery of the highly regio- and enantioselective macrocycle formation from the reaction of the unsymmetrical dialdehyde (*S*)-**4** with Lys in the presence of Zn^{2+} has prompted us to investigate the use of (*S*)-**4**+Zn^{2+} as a selective fluorescent probe for this unique unsymmetrical chiral diamine among various amino acids.

Using fluorescent probes for the detection of amino acids has been extensively studied because the fluorescence-based sensing provides advantages such as easily available instruments, high sensitivity and real-time analysis.[17] As an essential amino acid for human, L-Lys is involved in processes such as proteinogenesis, uptake of mineral nutrients, and fatty acid metabolism.[18,19] D-Lys is found to be important in various bacteria[20] and is also useful for the development of antimicrobial and antitubercular medicine.[21] Although a variety of fluorescent probes have been developed for Lys analysis,[22,23] very few reports on chemoselective as well as enantioselective detection of Lys were reported before.[24,25]

We have studied the fluorescence response of (*S*)-**4** toward both enantiomers of various common amino acids in the presence of Zn^{2+} under basic conditions. As shown in Figure 3, among 17 enantiomeric pairs of common amino acids, only L-Lys greatly enhances the fluorescence of (*S*)-**4** at λ_{emi} = 550 nm (λ_{exc} = 440 nm), but not D-Lys or all the other amino acid enantiomers.

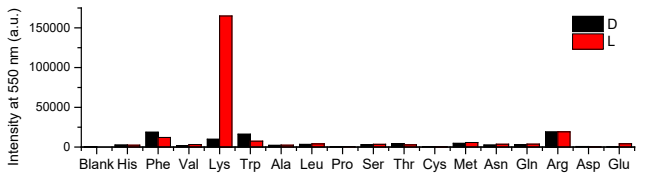

Figure 3. Fluorescence intensity at 550 nm of (*S*)-**4** (0.5 mM) + $Zn(OAc)_2$ (2.0 equiv) with 17 pairs of amino acid enantiomers (10 equiv) (λ_{exc} = 440 nm, slit: 1/1 nm. Solvent: CH_3CN/H_2O = 1/1 with 12.5 mM pH 8.4 buffer).

The effect of Lys concentration on the fluorescence of (*S*)-**4** was examined (Figure 4) (see Figure S84-S88 in SI for excitation and UV-vis spectra, and influences of Zn^{2+} and reaction time). Figure 4a compares the fluorescence spectrum of (*S*)-**4**+Zn^{2+} in the presence of L-Lys (10.0 equiv) with that of D-Lys (10.0 equiv). It gives a highly enantioselective fluorescent enhancement ratio [ef = $(I_L-I_0)/(I_D-I_0)$. I_0: the fluorescence intensity in the absence of D- and L-Lys] of 16.9. Figure 4b shows that as the concentration of L-Lys increases, the fluorescence intensity increases significantly initially and then reaches saturation at [L-Lys] ≥ 13 equiv. Whereas, D-Lys caused only very small fluorescence change over the entire concentration range (0 – 20 equiv). The limit of detection (LOD) for using (*S*)-**4** to detect L-Lys was found to be 1.41 × 10^{-7} M (Figure S89 in SI). A similar enantioselective fluorescence response for the interaction of (*S*)-**4** +Zn^{2+} with L- and D-Lys is also observed in DMSO/water (1:1) with 12.5 mM pH 8.4 buffer (See Figure S90 in SI). This probe can be used to determine the enantiomeric composition of Lys. (See Figure S91 and S92 in SI). The presence of other amino acids also does not significantly interfere the fluorescence response of (*S*)-**4** toward L-Lys in many cases (See Figure 97 and 98 in SI).

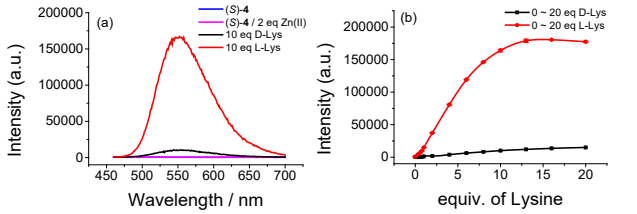

Figure 4. Fluorescence spectra of (*S*)-**4** (0.5 mM) + $Zn(OAc)_2$ (2.0 equiv) with D- and L-Lys (10.0 equiv). (b) Fluorescence intensity at 550 nm *versus* the equivalence of D- and L-Lys (error bars from three independent experiments. λ_{exc} = 440 nm. Slit: 1/1 nm. Solvent: CH_3CN/H_2O = 1/1 with 12.5 mM pH 8.4 buffer). (See full spectrum in Figure S93)

In conclusion, we have demonstrated for the first time that an unsymmetric chiral dialdehyde can undergo regio- and enantioselective macrocyclization with an unsymmetric chiral diamine through a dynamic imine transformation. It is also discovered that the presence of Zn^{2+} can further enhance the enantioselectivity in this process. This discovery has led to the development of a highly chemoselective as well as enantioselective fluorescent probe for the detection of lysine, an essential amino acid. It represents a new strategy to use the dynamic imine transformation to create structurally interesting and potentially useful materials.

ASSOCIATED CONTENT

Data Availability Statement

The data underlying this study are available in the published article and its Supporting Information.

Supplementary Information Available

Additional experimental procedures and spectroscopic data are provided.

AUTHOR INFORMATION

Corresponding Author

E-mail: lp6n@virginia.edu (Lin Pu)

ORCID

Lin Pu: 0000-0001-8698-3228

Notes

The authors declare no competing financial interest.

Acknowledgement

We thank the support of the US National Science Foundation (CHE-1855443 and CHE-2153466) for this project.

References

1. (a) C. D. Meyer, C. S. Joiner, J. F. Stoddart. Template-directed synthesis employing reversible imine bond formation. *Chem. Soc. Rev.*, **2007**, *36*, 1705. (b) M. Belowich, J. F. Stoddart. Dynamic imine chemistry. *Chem. Soc. Rev.*, **2012**, *41*, 2003-2024.
2. J. L. Segura, M. J. Mancheño, F. Zamora. Covalent organic frameworks based on Schiff-base chemistry: synthesis, properties, and potential applications. *Chem. Soc. Rev.*, **2016**, *45*, 5635-5671.
3. G. Zhang, M. Mastalerz. Organic cage compounds – from shape-persistency to function. *Chem. Soc. Rev.*, **2014**, *43*, 1934-1947.
4. D. Zhang, T. K. Ronson, J. R. Nitschke. Functional Capsules via Subcomponent Self-Assembly. *Acc. Chem. Res.*, **2018**, *51*, 2423-2436.

5. (a) J.-M. Lehn. Dynamic Combinatorial Chemistry and Virtual Combinatorial Libraries. *Chem. Eur. J.*, **1999**, *5*, 2455-2463. (b) P. T. Corbett, J. Leclaire, L. Vial, K. R. West, J.-L. Wietor, J. K. M. Sanders, S. Otto. Dynamic Combinatorial Chemistry. *Chem. Rev.*, **2006**, *106*, 3652-3711.
6. (a) N. E. Borisova, M. D. Reshetova, Y. A. Ustynyuk. Metal-Free Methods in the Synthesis of Macrocyclic Schiff Bases. *Chem. Rev.*, **2007**, *107*, 46-79. (b) S. Srimurugan, P. Suresh, B. Babu, H. N. Patic. Chiral Macrocyclic Schiff Bases: An Overview. *Mini-Reviews in Org. Chem*. **2008**, *5*, 228-24.
7. (a) A. Star, I. Goldberg, B. Fuchs. Dioxadiazadecalin/Salen Tautomeric Macrocycles and Complexes: Prototypal Dynamic Combinatorial Virtual Libraries. *Angew. Chem. Int. Ed.*, **2000**, *39*, 2685-2689. (b) J. Gawronski, H. Kolbon, M. Kwit, A. Katrusiak. Designing Large Triangular Chiral Macrocycles: Efficient [3 + 3] Diamine−Dialdehyde Condensations Based on Conformational Bias. *J. Org. Chem.*, **2000**, *65*, 5768-5773. (c) N. Kuhnert, A. M. Lopez-Periago. Synthesis of novel chiral non-racemic substituted trianglimine and trianglamine macrocycles. *Tetrahedron Lett.*, **2002**, *43*, 3329-3332. (d) M. Kwit, J. Gawrosky. Chiral calixsalen-type macrocycles from trans-1,2-diaminocyclohexane. *Tetrahedron: Asymmetry*, **2003**, *14*, 1303-1308. (e) N. Kuhnert, G. M. Rossignolo, A. López-Periago. The synthesis of trianglimines: on the scope and limitations of the [3 + 3] cyclocondensation reaction between (1R,2R)-diaminocyclohexane and aromatic dicarboxaldehydes. *Org. Biomol. Chem.*, **2003**, *1*, 1157-1170. (f) A. González-Álvarez, I. Alfonso, F. López-Ortiz, Á. Aguirre, S. García-Granda, V. Gotor. Selective Host Amplification from a Dynamic Combinatorial Library of Oligoimines for the Syntheses of Different Optically Active Polyazamacrocycles. *Eur. J. Org. Chem.*, **2004**, 1117.
8. (a) D. Beaudoin, F. Rominger, M. Mastalerz. Chiral Self-Sorting of [2 + 3] Salicylimine Cage Compounds. *Angew. Chem., Int. Ed.*, **2017**, *56*, 1244-1248. (b) D. Xu, R. Warmuth. Edge-Directed Dynamic Covalent Synthesis of a Chiral Nanocube. *J. Am. Chem. Soc.*, **2008**, *130*, 7520-7521. (c) T. Hasell, S. Y. Chong, K. E. Jelfs, D. J. Adams, A. I. Cooper. Porous Organic Cage Nanocrystals by Solution Mixing. *J. Am. Chem. Soc.*, **2012**, *134*, 588-598. (d) E. Jelfs Kim, X. Wu, M. Schmidtmann, J. T. A. Jones, J. E. Warren, D. J. Adams, A. I. Cooper. Large Self-Assembled Chiral Organic Cages: Synthesis, Structure, and Shape Persistence. *Angew. Chem.*, **2011**, *123*, 10841-10844.
9. (a) H. Brunner, H. Schiessling. Dialdehyde + Diamine Polymer or Macrocycle? *Angew. Chem., Int. Ed. Engl.*, **1994**, *33*, 125-126. (b) Z.B. Li, J. Lin, L. Pu. A cyclohexyl-1,2-diamine-derived bis(binaphthyl) macrocycle: Enhanced sensitivity and enantioselectivity in the fluorescent recognition of mandelic acid. *Angew. Chem. Int. Ed*. **2005**, *44*, 1690-1693.
10. M. Kwit, B. Zabicka, J. Gawronski. Synthesis of chiral large-ring triangular salen ligands and structural characterization of their complexes. *Dalton Trans.*, **2009**, *6783-6789*.
11. H. Tokunaga, K. Kazama, M. Tsuboi, M. Miyasaka. A novel Schiff base macrocycle based on 1,10-binaphthyl for fluorescence recognition. *Luminescence*, **2021**, *36*, 1561-1568.
12. P. Kovaricek, J.-M. Lehn. Merging Constitutional and Motional Covalent Dynamics in Reversible Imine Formation and Exchange Processes. *J. Am. Chem. Soc.*, **2012**, *134*, 9446-9455.
13. (a) Zhu, Y.; Wu, X.; Gu, S.; Pu, L. Free Amino Acid Recognition: A bisbinaphthyl-based fluorescent probe with high enantioselectivity. *J. Am. Chem. Soc*. **2019**, *141*, 175–181. (b) Y. Mao, M. Abed, N. B. Lee , X. Wu, G. Du and L. Pu. Determine Concentration and Enantiomeric Composition of Histidine by One Fluorescent Probe. *Chem. Commun*. **2021**, 57, 587-590.
14. Y. Mao, E. Thomae, S. Davis, C. Wang, Y. Li, L. Pu. One Molecular Probe with Opposite Enantioselective Fluorescence Enhancement at Two Distinct Emissions. *Org. Lett*. **2023**, *25*, 2157–2161.
15. Huang, Z.; Yu, S. S.; Yu, X. Q.; Pu. L. Zn(II) Promoted Dramatic Enhancement in the Enantioselective Fluorescent Recognition of Chiral Amines by a Chiral Aldehyde. *Chem. Sci.* **2014**, *5*, 3457-3462.
16. X. Wang, D. Shi, Y. Xu, S. Yu, F. Zhao, Y. Wang, L. Hu, J. Tian, X. Yu, L. Pu. Reaction of Zn(II) with a BINOL-Amino-Acid Schiff Base: An Unusual Off-On-Off Fluorescence Response. *Tetrahedron Lett*. **2018**, 59 2332–2334.
17. (a) Pu, L. Enantioselective Fluorescent Recognition of Free Amino Acids: Challenges and Opportunities. *Angew. Chem. Int. Ed*. **2020**, *59*, 21814-21828. (b) Zhou, Y.; Yoon, J. Recent Progress in Fluorescent and Colorimetric Chemosensors for Detection of Amino Acids. *Chem. Soc. Rev*. **2012**, *41*, 52–67. (c) Wang, J.; Liu, H.-B.; Tong, Z.; Ha, C.-S. Fluorescent/Luminescent Detection of Natural Amino Acids by Organometallic Systems. *Coord. Chem. Rev*. **2015**, *303*, 139-184.
18. Wu, G. Amino acids: metabolism, functions, and nutrition. *Amino Acids* **2009**, *37*, 1–17.
19. *Tomé, D.; Bos, C.* Lysine requirement through the human life cycle. *J. Nutrition **2007**, 137, 1642S–1645S.*
20. (a) Miyamoto, T.; Homma, H. D-Amino acid metabolism in bacteria. *J. Biochem*. **2021**, *170*, 5–13. (b) Zabriskie, T. M.; Jackson, M. D. Lysine biosynthesis and metabolism in fungi. *Nat. Prod. Rep*. **2000**, *17*, 85–97.
21. Verma, D. P.; Ansari, M. M.; Verma, N. K.; Saroj, J.; Akhtar, S.; Pant, G.; Mitra, K.; Singh, B. N.; Ghosh, J. K. Tandem Repeat of a Short Human Chemerin-Derived Peptide and Its Nontoxic D-Lysine-Containing Enantiomer Display Broad-Spectrum Antimicrobial and Antitubercular Activities. *J. Med. Chem.* 2021, 64, 20, 15349–15366
22. (a) Yang, B.; Zhou, J.; Huang, X.; Chen, Z.; Tian, S.; Shi, Y. A New Pyrroloquinoline-Derivative-Based Fluorescent Probe for the Selective Detection and Cell Imaging of Lysine. *Pharmaceuticals* **2022**, *15*, 474. (b) Ma, H.; Qi, C.; Cao, H.; Zhang, Z.; Yang, Z.; Zhang, B.; Chen, C.; Lei, Z.Q. Water-soluble fluorescent probes for selective recognition of lysine and its application in an object carry-and-release system. *Chem. Asian J.* **2016**, *11*, 58–63. (c) Zhou, Y.; Won, J.; Lee, J.Y.; Yoon, J. Studies leading to the development of a highly selective colorimetric and fluorescent chemosensor for lysine. *Chem. Commun.* **2011**, *47*, 1997–1999. (d) Lohar, S.; Safin, D. A.; Sengupta, A.; Chattopadhyay, A.; Matalobos, J.S.; Babashkina, M.G.; Robeyns, K.; Mitoraj, M.P.; Kubisiak, P.; Garcia, Y.; Das, D. Ratiometric sensing of lysine through the formation of the pyrene excimer: Experimental and computational studies. *Chem. Commun*. **2015**, *51*, 8536–8539.
23. (a) Adhikari, S.; Ghosh, A.; Mandal, S.; Guria, S.; Banerjee, P.P.; Chatterjee, A.; Das, D. Colorimetric and fluorescence probe for the detection of nano-molar lysine in aqueous medium. *Org. Biomol. Chem*. **2016**, *14*, 10688–10694. (b) Yang, L.; Xie, Y.; Chen, Q.; Zhang, J.; Li, L.; Sun, H. Colorimetric and fluorescent dual-signal chemosensor for lysine and arginine and its application to detect amines in solid-phase peptide synthesis. *ACS Appl. Bio Mater*. **2021**, *4*, 6558–6564. (c) Zhu, Z.; Wang, Y.; Ding, H.; Fan, C.; Tu, Y.; Liu, G.; Pu, S. A novel full symmetric diarylethene-based ratiometric fluorescent sensor for lysine and the application for a logic circuit. *Luminescence* **2021**, *36*, 691–697. (d) Hou, J.-T.; Li, K.; Liu, B.-Y.; Liao, Y.-X.; Yu, X.-Q. The first ratiometric probe for lysine in water. *Tetrahedron* **2013**, *69*, 2118–2123. (e) Qian, X.; Gong, W.; Wang, F.; Lin, Y.; Ning, G. A pyrylium-based colorimetric and fluorimetric chemosensor for the selective detection of lysine in aqueous environment and real sample. *Tetrahedron Lett*. **2015**, *56*, 2764–2767. (f) K. Secor, J. Plante, C. Avetta, T. Glass. Fluorescent sensors for diamines. *J. Mater. Chem*. **2005**, *15*, 4073–4077.
24. Du, G.; Pu, L. Micelle-encapsulated fluorescent probe: Chemoselective and enantioselective recognition of lysine in aqueous solution. *Org. Lett*. **2019**, *21*, 4777–4781.
25. Yang, J.; Jiang, L.; Tian, J.; Yu, S.; Yu, X.; Pu, L. Fluorous Phase-Enhanced Fluorescent Sensitivity for Enantioselective Recognition of Lysine. *Org. Lett.* **2022**, *24*, 9327–9331.